

Experimental demonstration of quantum state tomography applied to dopant ions in a solid

J. J. Longdell and M. J. Sellars

Laser Physics Center, Research School of Physical Sciences and Engineering,
Australian National University, Canberra, ACT 0200, Australia.

(Dated: August 29, 2002)

We report on the implementation of quantum state tomography for an ensemble of Eu^{3+} dopant ions in a Y_2SiO_5 crystal. The tomography was applied to a qubit based on one of the ion's optical transitions. The qubit was manipulated using optical pulses and measurements were made by observing the optical free induction in a phase sensitive manner. Fidelities of $> 90\%$ for the combined preparation and measurement process were achieved. Interactions between the ions due to the change in the ions' permanent electric dipole moment when excited optically were also measured. In light of these results, the ability to do multi-qubit quantum computation using this system is discussed.

Rare earth ions doped into inorganic crystals are promising candidates for demonstrating quantum computing operations [1, 2, 3]. The properties that make rare earth ion-doped crystals amenable for quantum computing demonstrations include:

1. Optical transitions with long coherence times, up to 2.6 ms, have been observed [4].
2. Long coherence times in their ground state nuclear spin transitions, up to 60 ms, have been observed [5].
3. Strong coupling between the electronic states and nuclear spin states enables the optical manipulation and readout of the spin states [6, 7].
4. Large inhomogeneous broadening in the optical transitions, typically GHz, enables many homogeneously broadened ensembles or even single ions to be addressed individually [4].
5. Strong electric dipole-dipole interactions (as large as GHz) enabling coupling between the ions [8].

Here we demonstrate the ability to address a selected subset of the ions, place their states at any given point on the Bloch sphere and then read out their states using a sequence of optical pulses. We also characterize the interaction between different subsets of ions. From the results we determine conditions required to demonstrate two qubit operations.

The setup used was similar to that used in [1]. A highly stabilized dye laser was used with an established stability of better than 200 Hz over timescales of 0.2 s. The light incident on the sample was gated with two acousto-optic modulators (AOMs) in series. These allowed pulses with an arbitrary amplitude and phase envelope to be applied to the sample. The overall frequency shift introduced by the AOMs was 10 MHz. The transmitted light was combined with an unshifted laser beam in a Mach-Zehnder interferometer. The beat signal detected with a photo-diode was combined in phase and quadrature with

a 10 MHz reference to allow phase sensitive detection. In addition to the setup of [1] an auxiliary optical beam and radio frequency (RF) fields were used to repump the ground state hyperfine levels. The measurements were carried out with the crystal in the temperature range 3-5 K.

The Y_2SiO_5 sample had 0.5 at.% europium, which sits at the yttrium sites in the lattice. There are two stable isotopes of europium of near equal abundance and there are two different crystallographic sites for yttrium in the lattice. The experiment was performed on ^{151}Eu ions that substituted for yttrium at site 1 [9].

Applying optical pulses of definite area requires that all the ions experience the same generalized Rabi frequency. This requirement is problematic for a number of reasons. It requires the spread in resonance frequencies of the ions (c. 10 GHz for the whole sample) to be much smaller than the on-resonance Rabi frequency (c. 500 kHz available with 200 mW of laser power). It also requires that all ions have the same oscillator strength, which means that the resonant transition must be from the same ground state hyperfine level to the same excited state hyperfine level for all the ions. Further to these it also requires illuminating all the ions with the same intensity of light rather than the normal Gaussian laser beam profile.

Optical holeburning techniques similar to those introduced by Pryde et al. [1] were used to isolate a subset of ions to which accurate area pulses could be applied. All the ions that were not wanted in the subset of ions and that had a resonance close to the laser were optically pumped to another hyperfine level and thus far from resonance with the laser. The procedure was as follows: First all ions with a resonance close to the laser frequency were optically pumped to another hyperfine level. Then one RF field and the auxiliary optical beam was applied to the sample. The RF field was swept in frequency 34.51 MHz and the auxiliary optical beam was shifted from the laser frequency by 85.9 MHz. The effect was to repump the ^{151}Eu ions with the $5=2 \rightarrow 5=2$ transition frequency close to that of the laser into the $5=2$ ground state. These transitions are shown on the

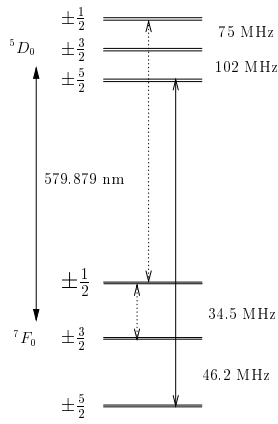


FIG . 1: Energy level diagram for ^{151}Eu at site 1. The experiment was performed on the $5=2 \rightarrow 7=2$ transition. The RF and optical fields used for burning back are shown with dotted lines

energy level diagram, FIG . 1.

This resulted in a 300 kHz wide feature with a Lorentzian-like lineshape. This was then narrowed to a 50 kHz feature with a rectangular lineshape by applying 'zero area pulses' to the ions. The laser beam is modulated with an envelope given by the difference of two sinc ($\sin(x)/x$) functions. The lengths and amplitudes of the two sinc functions were chosen to excite the ions with a resonance frequency within 500 kHz of the laser apart from those within 25 kHz of the laser.

The spread in the optical frequencies of the subset was then narrow compared to the available resonant Rabi frequencies, however because of the spatial distribution of intensity across the laser beam we don't yet have an ensemble to which we can apply precise area pulses.

To select out ions in a particular region of the laser beam, a series of 4 μs long pulses were applied to the sample, some of the ions experienced a π pulse and were left in the ground state, ions that saw a different intensity were pumped to a different hyperfine level. Ten π pulses were applied with an 8 ms delay between them to allow the excited ions to decay. Afterwards it could be concluded from the free induction decays for various pulse lengths that the Rabi frequency spread of the ensemble was of the order of 10%.

The pulse sequence used for the tomography consisted of three pulses each separated by 70 μs . First a pulse of a particular length and phase was applied. This was followed by a π pulse unshifted in phase, to rephase the inhomogeneous broadening in the sample. At $t = 140 \mu\text{s}$ a π pulse was applied that was also unshifted in phase. The axes for the Bloch vectors were chosen such that the ground state ($|j=0\rangle$) was along the negative z axis and laser pulses that were unshifted in phase caused rotations about the y axis.

The first pulse was used to create an arbitrary state, and the coherent emission resulting from this and the

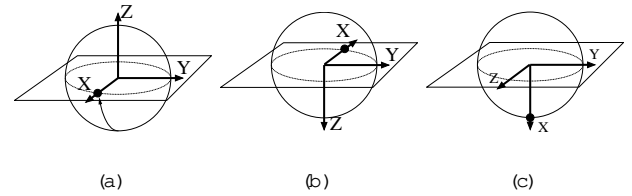


FIG . 2: The effect of the tomography sequence on the Bloch sphere for the case where the preparation pulse is a π pulse. Experimental results for a shot of this type are shown in FIG . 3. (a) The state is moved to the equator by the first pulse in the sequence. This gives coherent emission out of phase with the laser. (b) Just before $t = 140 \mu\text{s}$ the system rephases on the opposite side of the Bloch sphere, giving coherent emission in phase with the laser. (c) The final π pulse rotates the state to the ground state, which results in no coherent emission.

rest of the sequence constituted a measurement of this state. The first pulse was therefore viewed as causing a rotation of the state vector on the Bloch sphere and the following two pulses viewed as a rotation of both the state vector and the Bloch sphere itself. At each point the coherent emission measures the projection of the state onto the horizontal plane. Thus the amplitude of the component of the emission after the first pulse that was in phase (in quadrature) with the laser was proportional to $\langle X | \rho | X \rangle$ ($\langle Y | \rho | Y \rangle$) for the initial state. This coherent emission decayed over 20 μs ($1/(50 \text{ kHz})$) due to the inhomogeneous linewidth of the ensemble. The ensemble rephased at 140 μs and at that time a π pulse was applied. As the ensemble was rephasing before the π pulse the amplitude of the emission in phase (in quadrature) with the laser was proportional to $\langle X | \rho | X \rangle$ ($\langle Y | \rho | Y \rangle$) for the initial state. After the π pulse the amplitude of the emission in phase (in quadrature) with the laser was proportional to $\langle Z | \rho | Z \rangle$ ($\langle Y | \rho | Y \rangle$) for the initial state. These measurements overdetermine the initial Bloch vector, and linear least squares was used to extract the measured Bloch vector. The length of the Bloch vector was calibrated using two particular input states: ($|j=1\rangle + |j=0\rangle$) prepared using a π pulse unshifted in phase and $|j=0\rangle$ prepared by not having a preparation pulse.

The density is given by $\rho = \sum_j |j\rangle \langle j|$, where $|j\rangle$ is the input state and ρ is the measured density matrix. A significant contribution to the error in the tomography process was the shot to shot variation in the number of ions to which the process was applied. The requirement of phase coherence for the 200 μs of the tomography sequence was easily satisfied by the laser. However the preparation of the spike took approximately 10 μs , leading to the possibility that the laser drifts a significant fraction of the 50 kHz width of the spike in this time. This caused a shot to shot variation in the number of ions to which the tomography was applied which in turn had the

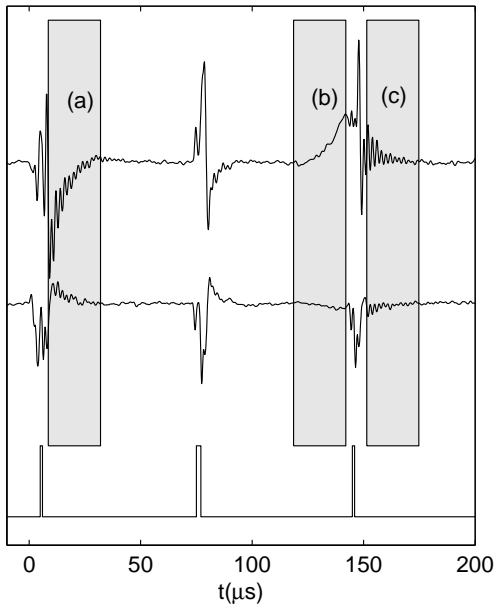


FIG . 3: The results of a quantum state tomography sequence. In the top trace the amplitude of the coherent emission in phase with the applied light is plotted versus time. The second trace shows the component in quadrature with the applied light. The applied optical pulses saturate the detector which takes 10 ns to recover. The positions of the applied light pulses as shown schematically in the third trace. The labels (a), (b) and (c) correspond the snapshots of the Bloch spheres shown in FIG . 2. The regions over which the signal was integrated to arrive at measurements are shown in gray.

TABLE I: Fidelity of the combined state preparation and tomography for different input states. Each point was repeated three times and the fidelities reported are the worst of those repeats. The position of the last state on the Bloch sphere corresponds to the position of Canberra on the earth.

State	Fidelity	Fidelity assuming pure state
$(j_i + i j_l\rangle) = \frac{p}{2}$	0.95	0.95
$(j_i + j_l\rangle) = \frac{p}{2}$	0.95	0.95
$ j_i\rangle$	0.96	0.97
$(j_i - j_l\rangle) = \frac{p}{2}$	0.96	0.97
$ j_l\rangle$	0.88	0.89
$(j_i - i j_l\rangle) = \frac{p}{2}$	0.88	0.96
$\cos(0.960) j_i + \sin(0.960)\exp(2.60i) j_l\rangle$	0.81	0.99

effect of scaling the length of the measured Bloch vector. If a state that is being measured can be assumed to be pure, the measured Bloch should be normalized. This normalization makes the tomography process insensitive to drifts in the number of ions to which the process is applied. This leaves the inhomogeneity in the Rabi frequencies as the main source of error in the process.

The fidelity of the combined state preparation and tomography are shown in table I.

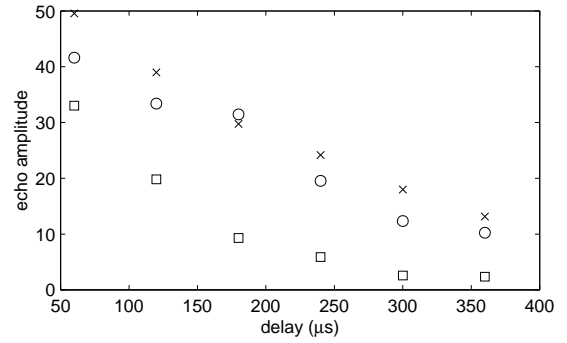


FIG . 4: A photon echo sequence was applied to a spike, during the sequence a perturbing pulse is applied to another spike prepared 5 MHz away. The echo amplitude vs delay between the two applied pulses. The crosses correspond to no perturbing pulse, the circles a perturbing pulse applied just after the $\pi/2$ pulse and the squares just after the π pulse.

The results of one particular experimental shot are shown in FIG . 3. Here the state to be measured is created at $t = 0$ with a $\pi/2$ pulse unshifted in phase. This puts the Bloch vector along the x axis. This gave coherent emission out phase with the laser, this decayed as the inhomogeneous broadening dephases the ensemble. At $t = 70\text{ ns}$ the π pulse was applied to rephase the inhomogeneous broadening, this should have caused no polarization of the ions and thus produced no coherent emission. As $t = 140\text{ ns}$ approaches the ensemble rephases on the opposite side of the Bloch sphere producing coherent emission in phase with the laser. At $t = 140\text{ ns}$ a $\pi/2$ pulse was applied which takes the ions down to the ground state, stopping the coherent emission. The high frequency ringing superimposed on the emission following the application of the pulses is due to them exciting the edges of the trenches in which the spikes lie.

We also measured interaction between the europium ions. Each europium ion in $\text{Eu:Y}_2\text{SiO}_5$ has a permanent electric dipole moment, which changes by a few percent when the ion is excited optically. A europium ion will see a change in electric field and hence its resonant frequency changes when a nearby ion is excited [8].

This interaction is large for ions that are close, however when working with two ensembles each of which constitute a small fraction of the inhomogeneous line, the distance from a particular member of one ensemble to any member of the other is much larger than the crystal's mean inter-dopant separation. Because of the random nature of the relative positions of a given pair of ions the excitation of one ensemble causes a random shift in the resonance frequencies of each of the members of the other.

In order to measure the frequency shifts in one ensemble due to the excitation of another a photon echo sequence is applied to a spike. During the sequence a perturbing pulse is applied to another spike prepared 5 MHz

away. When the perturbing pulse was applied just after the pulse the amplitude of the echo was reduced significantly. When the perturbing pulse was applied just after the $\pi/2$ pulse the reduction in the amplitude of the echo was much smaller. This confirms that the perturbing pulse induces a frequency shift which, if applied at the start of the sequence, is rephased.

From FIG. 4 we can see that the excitation of the perturbing ensemble causes a spread of ~ 1 kHz (~ 200 s) in the resonant frequencies. The ensemble to which the perturbing pulses were applied was prepared by burning a trench and then burning back an antihole. This ~ 300 kHz wide feature has approximately 10^6 of the ions. This corresponds to a mean inter-dopant separation 100 times greater than for the full ensemble or $100 \times 25 = 2500$ nm. As we can expect the interaction to scale as r^{-3} , ions separated by the mean inter-europium distance in this sample can be expected to see shifts of ~ 1 GHz.

In order to do multi-qubit quantum computation, in addition to the other forms of inhomogeneity that were overcome in this work, one would have to overcome the problem of inhomogeneity in ion-ion interaction strength. When working with two spikes in the inhomogeneous line the mean shift of frequencies in one ensemble is a small percentage of the others inhomogeneous linewidth. This makes the method of Ohlsson et. al. [3] for overcoming interaction strength inhomogeneity very difficult to implement as it relies on selecting ions pairs with frequency shifts greater than the inhomogeneous linewidth of the ensembles. However if one has the ability to perform accurate single qubit operations on the ensembles the interactions need only be large compared to the homogeneous linewidths. The pulse sequence would be similar to that used to measure the interactions except at the end of the sequence it all the ions that have experienced a particular phase shift due to the interaction would be taken back to the ground state, leaving the others to some extent excited. Repeated application of such a pulse sequence would optically pump all the ions from the ensemble except those with the desired interaction strength. While this would leave ensembles with more ions than would the Ohlsson scheme the number of ions left however would still decrease rapidly with the number of qubits making such an approach not scalable.

The problem of inhomogeneity of ion-ion interaction strength could be overcome using "molecules", that is a large number of identical ensembles, in the same way as in liquid state NMR quantum computing. At present however, no such materials present themselves. The detection of single ions would also solve this problem. The optical detection of single impurity sites in solids has been demonstrated [10], although the low oscillator strengths for rare earths and the requirement that the detection be spin selective would make the task more difficult. In the authors' opinion this compares favorably with the situa-

tion for other schemes for the detection of single qubits in solids.

In conclusion we have demonstrated quantum state tomography on Eu^{3+} dopant ions in Y_2SiO_5 , with fidelities of typically $> 90\%$ achieved. We also measured the frequency shifts of one ensemble of dopant ions caused by the excitation of another group of dopant ions. Further to this the ions have optically resolvable hyperfine structure where the coherence can be stored in states insensitive to electric dipole-dipole interactions.

The detection of the spin state of single ions would solve the problem of inhomogeneity in the ensembles enabling multi quantum computing, with significantly higher fidelities than demonstrated here.

While scalable quantum computing using ensembles selected from the inhomogeneous line will not be possible, demonstrations for small numbers of qubits are feasible. The results in the paper show we can achieve high enough fidelity for the single qubit operations on 50 kHz spikes. We have also shown that ensembles of the order of 300 kHz wide are required for the ensembles to have sufficiently strong interactions.

We were restricted to working with Rabi frequencies of 250 kHz by the bandwidth of the modulation system used to apply the pulses and the available laser power. Intensities of 200 W/cm^2 are needed for 250 kHz Rabi frequencies. It is envisioned that the use of moderately higher laser powers, smaller spot sizes, improvements to the modulation system and perhaps the use of composite pulse sequences will allow the use of higher Rabi frequencies. These higher Rabi frequencies would allow the demonstration of two qubit operations for ensembles of ions.

The authors would like to thank George Pryde and Neil Mansson for their helpful comments on the manuscript.

Electronic address: jevon.longdell@anu.edu.au

- [1] G. J. Pryde, M. J. Sellars, and N. B. Mansson, *Phys. Rev. Lett.* **84**, 1152 (2000).
- [2] K. Ichimura, *Optics Comm.* **196**, 119 (2001).
- [3] N. Ohlsson, R. K. M. Chan, and S. Kroll, *Optics Comm.* **201**, 71 (2002).
- [4] R. W. E. Quall, Y. Sun, R. L. Cone, and R. M. Macfarlane, *Phys. Rev. Lett.* **72**, 2179 (1997).
- [5] Elliot Fraval, Personal Communication.
- [6] J. Mlynec, N. C. Wong, R. G. DeVoe, E. S. Kintzer, and R. G. Brewer, *Phys. Rev. Lett.* **50**, 993 (1983).
- [7] L. E. Erickson, *Opt. Comm.* **21**, 147 (1977).
- [8] F. R. G. Raab, A. Renn, G. Zumofen, and U. P. Wild, *Phys. Rev. B* **58**, 5462 (1998).
- [9] R. Yano, M. Mitsuanga, and N. Uesugi, *Opt. Lett.* **16**, 1884 (1991).
- [10] A. G. Gubler, A. D. Rabenstein, C. Tietz, L. Fleury, J. Warchrup, and C. von Borczyskowski, *Science* **276**, 2012 (1997).